Microscopy and Microanalysis (2019), 1–10
doi:10.1017/S1431927618015520

Microscopy AND Microanalysis

Original Article

Noninvasive Continuous Monitoring of Adipocyte Differentiation: From Macro to Micro Scales

Maayan Lustig[1], Qingling Feng[2], Yohan Payan[3], Amit Gefen[1] and Dafna Benayahu[4]*

[1]Department of Biomedical Engineering, Faculty of Engineering, Tel Aviv University, Tel Aviv 6997801, Israel; [2]Key Laboratory of Advanced Materials of Ministry of Education of China, School of Materials Science and Engineering, Tsinghua University, Beijing 100084, China; [3]CNRS, Grenoble INP, TIMC-IMAG, University of Grenoble Alpes, Grenoble F-38000, France and [4]Department of Cell and Developmental Biology, Sackler School of Medicine, Tel Aviv University, Tel Aviv 6997801, Israel

Abstract

3T3-L1 cells serve as model systems for studying adipogenesis and research of adipose tissue-related diseases, e.g. obesity and diabetes. Here, we present two novel and complementary nondestructive methods for adipogenesis analysis of living cells which facilitate continuous monitoring of the same culture over extended periods of time, and are applied in parallel at the macro- and micro-scales. At the macro-scale, we developed visual differences mapping (VDM), a novel method which allows to determine level of adipogenesis (LOA)—a numerical index which quantitatively describes the extent of differentiation in the whole culture, and percentage area populated by adipocytes (PAPBA) across a whole culture, based on the apparent morphological differences between preadipocytes and adipocytes. At the micro-scale, we developed an improved version of our previously published image-processing algorithm, which now provides data regarding single-cell morphology and lipid contents. Both methods were applied here synergistically for measuring differentiation levels in cultures over multiple weeks. VDM revealed that the mean LOA value reached 1.11 ± 0.06 and the mean PAPBA value reached >60%. Micro-scale analysis revealed that during differentiation, the cells transformed from a fibroblast-like shape to a circular shape with a build-up of lipid droplets. We predict a vast potential for implementation of these methods in adipose-related pharmacological research, such as in metabolic-syndrome studies.

Key words: adipogenesis, morphology, lipid droplets, image processing, mapping

(Received 24 June 2018; revised 15 October 2018; accepted 1 November 2018)

Introduction

Cell cultures of adipocytes frequently serve as model systems for the research of adipose tissue-related diseases, such as obesity and diabetes and in tissue engineering studies seeking reconstruction (Patrick, 2000; Steppan et al., 2001; Furukawa et al., 2004; Choi et al., 2010). 3T3-L1 is a mesenchymal cell line that is commonly used to study transcription regulation and cell–cell/cell–substrate interactions that are required for adipogenesis (Poulos et al., 2010). *In vitro* analysis of these cells employs staining techniques, for instance—lipid droplet (LD) staining using reagents such as Oil-Red O, BODIPY 493/503 on fixed cultures, providing a snapshot of the specific time point (Ramírez-Zacarías et al., 1992; Ross, 2000; Murphy et al., 2010; Harris et al., 2013; Qiu & Simon, 2016). The stained cultures are typically used for evaluating the extent of adipocyte differentiation (Deutsch et al., 2014). Adipogenesis can be also evaluated indirectly by extraction of the lipid content using spectrophotometer analyses of dye color absorbance (Choi et al., 2009). The measurements of lipid content or LDs quantitation (number and size) are important features that allow us to follow and analyze various drug effects on adipogenesis (Ejaz et al., 2009; Lin et al., 2009; Or-Tzadikario et al., 2010; Levy et al., 2012; Shoham et al., 2012; Shoham & Gefen, 2012*a*, 2012*b*; Mor-Yossef Moldovan et al., 2018; Lustig et al., 2018*a*, 2018*b*).

When examining the level of adipogenic differentiation in cultures using any of the methods described above, the cultures need to be fixed and terminated. Hence, further or ongoing observations are not feasible past the time point of measurement, which is clearly counterproductive in terms of statistical power and hence cost management of experiments. Our group previously presented an image-processing-based technique for objectively and quantitatively measuring LD sizes in adipocyte cultures, monitored using digital phase-contrast microscopy over time (Or-Tzadikario et al., 2010). This aforementioned method measures the amount of lipid contents per field of view (FOV), and further assesses numbers and sizes of LDs; however, the program is not designed to extract morphological data.

In this article, we build upon our previous research record in the field of adipocyte research (Or-Tzadikario et al., 2010; Shoham & Gefen, 2011, 2012*a*, 2012*b*; Levy et al., 2012; Shoham et al., 2012, 2014, 2015; Ben-Or Frank et al., 2015; Katzengold et al., 2015; Mor-Yossef Moldovan et al., 2018; Lustig et al., 2018*a*, 2018*b*) and present progress in the form of two innovative and complementary nondestructive methods that are applied at the macro- and micro-scales for adipogenesis analysis. At the macro-scale, we developed a new method for

***Author for correspondence:** Dafna Benayahu, E-mail: dafnab@tauex.tau.ac.il

Cite this article: Lustig M, Feng Q, Payan Y, Gefen A, Benayahu D (2019) Noninvasive Continuous Monitoring of Adipocyte Differentiation: From Macro to Micro Scales. *Microsc Microanal*. doi:10.1017/S1431927618015520

mapping the level of adipogenesis (LOA) on a whole culture based on the morphological changes that are apparent between differentiation stages of adipogenesis. At the micro-scale, we present an improved version of the image-processing algorithm (Or-Tzadikario et al., 2010), which offers substantially greater accuracy when analyzing lipid content and the ability to extract data regarding single-cell shape, which are important features characterizing the differentiation process. Both techniques facilitate objective quantification of adipocyte cultures monitored using phase-contrast microscopy over time. To demonstrate the utility and versatility of the two methods described here, we employed both in measuring differentiation levels in 3T3-L1 cells over 19 days.

Development of in vitro methods that enable the study of living model systems (including cell culture models) allow for better design of experimental protocols in adipose cell research and tissue engineering, and is eventually useful for gaining clearer understanding of the pathophysiology of diseases, such as type II diabetes or osteoporosis. We therefore see the present work as one which may ultimately pave the way for clinical management and drugs development for these conditions, through statistically powered, cost-effective quantitative methodological research.

Materials and Methods

Cell Cultures

Mouse embryonic 3T3-L1 preadipocytes (American Type Culture Collection, Manassas, Virginia, USA) were cultured on square-shaped glass coverslips (2 cm × 2 cm) at a density of 1×10^4 cells/cm^2. The growth medium consisted of high-glucose Dulbecco's modified Eagle's medium (450 mg/dL; Biological Industries, Kibbutz Beit-Haemek, Israel), 10% fetal bovine serum (Biological Industries, Kibbutz Beit-Haemek, Israel), 1% L-glutamine (Biological Industries), 0.1% penicillin–streptomycin (Sigma, Sigma-Aldrich, Rehovot, Israel), and 0.5% 4-(2-hydroxyethyl)-1-piperazineethane-sulfonic acid (Sigma). The GM was changed twice a week (Shoham et al., 2012, 2015).

Differentiation was induced when the cultures reached a confluence of ∼90% based on a protocol as previously published (Shoham et al., 2012, 2015).

Macro-Scale, Visual Differences Mapping

3T3-L1 cells are fibroblast cells that change phenotype during differentiation; the cells become round and are occupied mostly with LDs, as is characteristic to adipogenic differentiation. The accumulation of LDs in the adipocyte cells was noted and quantified at the macro-scale throughout the entire culture period using a new adipogenesis mapping method, developed as described here. Visual differences mapping (VDM) allowed for the evaluation of LOA in the living cultures over the period of experimentation, using phase-contrast microscopy (TMS-F; Nikon, Tokyo, Japan). Triplicates were used in all these experiments ($n = 3$).

Transparent millimetric (grid/matrix) stickers were pasted on the outer bottoms of tissue culture plates to introduce identical observation squares of 1 mm × 1 mm area, in which the cells and grid lines could be viewed in one focal plane and the whole observation square is in the same FOV when observing the culture at a microscope magnification of ×40. Mapping of the cell cultures was performed continuously throughout the culturing period to analyze the levels of differentiation from fibroblasts to adipocytes (Figs. 1a–c).

Culture Mapping and Evaluation

The mapping process relies on quantitative evaluation of cell states at each of the 1 mm × 1 mm squares, which yields the local LOA grading and the distribution of grades as follows. Evaluation grades are defined between 0 and 4, with a grade of "0" denoting only fibroblasts in the square and no differentiated adipocytes (Fig. 1d). A grade of "1" indicates that more than 0% and up to 25% of the square area (inclusive) is covered by differentiated adipocytes. A grade of "2" indicates that more than 25% and up to 50% of the square area (inclusive) is covered by differentiated adipocytes. A grade of "3" indicates that more than 50% and up to 75% of the square area (inclusive) is covered by differentiated adipocytes. A grade of "4" indicates that more than 75% of the square area is covered by differentiated adipocytes, and the remaining area is covered by fibroblasts (Fig. 1d). Following this mapping, an adipogenesis-map is created; the resulting map displays the LOA in the culture throughout the experiment. The diagram illustrates the location and proportion of areas covered by differentiated adipocytes in the culture at different time points.

Additionally, a square area solely containing fibroblasts is considered as "NO", while a square area containing adipocytes at any differentiation level is considered as "YES" (Fig. 1e), consistent with the ranking system.

The above mapping over the whole culture is performed continuously without the need to take photographs of the culture. The examiner observes the culture and assigns suitable grades to each square delineated by the grid. In order to minimize variability across examiners (i.e., inter-rater variability), the grades were determined as follows: 20 photographs of sampled squares were taken (e.g., as in Fig. 1b), each picture representing a different level of adipogenic differentiation. Five examiners were individually asked to rank the area populated by differentiated adipocytes in each photographed square. According to these ranking assignments, LOA values were classified into five evaluation options.

It is worthwhile to note that there is a major visual difference between fibroblasts and adipocytes, even at an early stage of differentiation; during differentiation, the cells change their shape from a spindle fibroblast-like shape to a round adipocyte with accumulated LDs (Mor-Yossef Moldovan et al., 2018; Lustig et al., 2018*a*, 2018*b*). The visual differences between these two cell types was apparent at all light intensities of the microscope and this is consistent with our earlier studies (Or-Tzadikario et al., 2010; Shoham & Gefen, 2011, 2012*a*, 2012*b*; Levy et al., 2012; Shoham et al., 2012, 2014, 2015; Ben-Or Frank et al., 2015; Katzengold et al., 2015; Mor-Yossef Moldovan et al., 2018; Lustig et al., 2018*a*, 2018*b*).

Mean level of adipogenesis. A mean value for the LOA is calculated for each culture using the following (weighted average) equation [Equation (1)]:

$$\text{mean LOA} = \frac{\sum_{i=0}^{4} (i \cdot N_i)}{N}, \tag{1}$$

where N_i is the number of squares with the LOA grade i and N is the total number of squares.

The mean LOA value provides an evaluation of adipogenic differentiation of an entire culture. The LOA evaluation values of each square (ranged between 0 and 4) are recorded in Excel

https://doi.org/10.1017/S1431927618015520

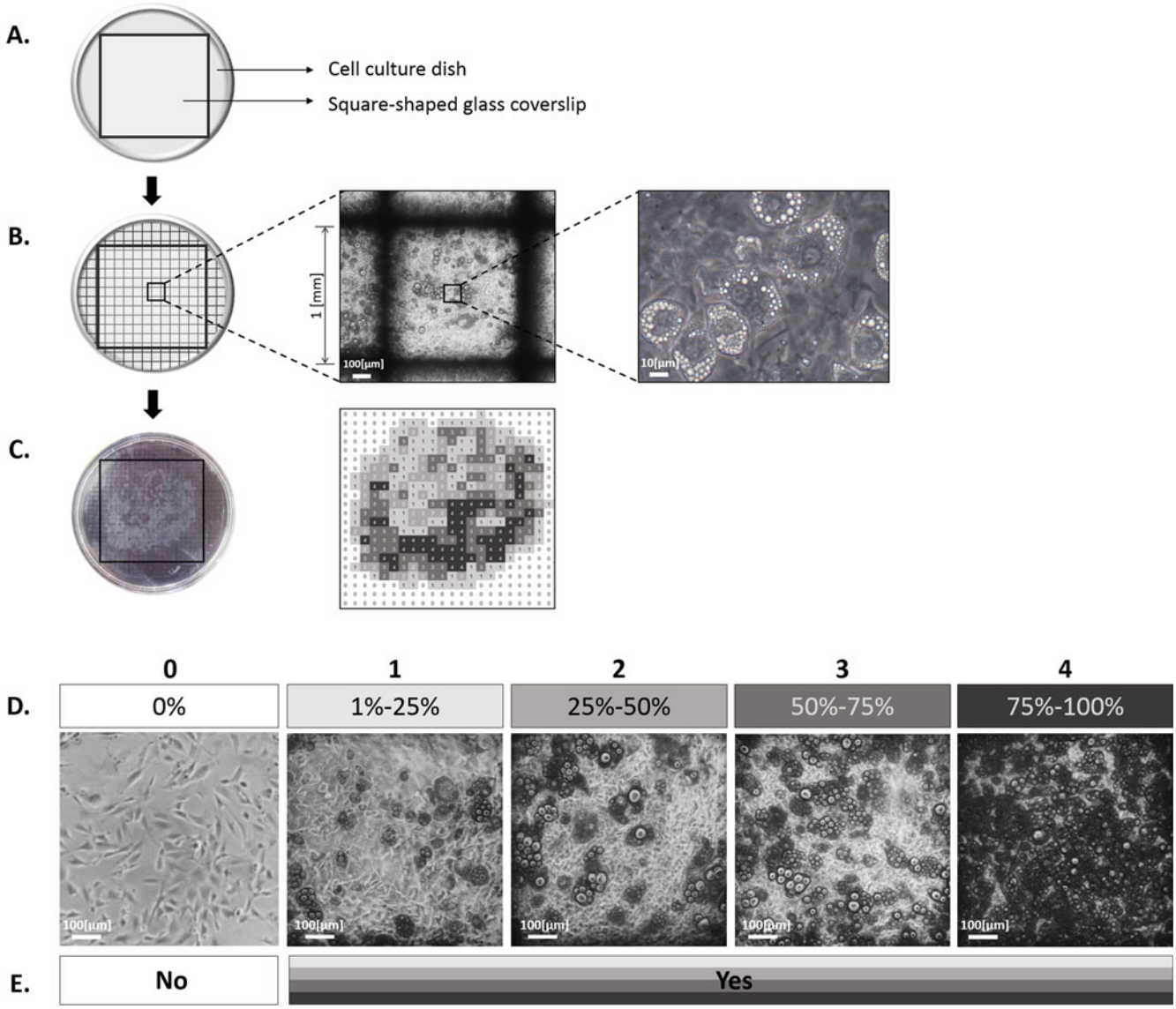

Fig. 1. The visual differences mapping (VDM) facilitates a macro-scale assessment of cell cultures, specifically in mapping the propagation of the adipogenesis differentiation pattern. **a**: An illustration of a cell culture, seeded on a glass coverslip placed in a dish. **b**: The cell culture with the VDM gridded sticker pasted on the outer bottom of the dish; the grid lines are visible through the transparent glass coverslip. Micrograph at ×40 magnification: The differentiated/nondifferentiated cells are visible between the grid lines. Mature adipocytes (containing lipid droplets, LDs) at ×400 magnification; fibroblasts are also visible in the vicinity. **c**: The resulting adipogenesis map, obtained using VDM. **d**: VDM data analysis: Grading the level of adipogenesis (LOA); values are between 0 and 4, the specific value indicates the extent of the area covered by differentiated adipocytes. **e**: Percentage area populated by adipocytes (PAPBA), which is the percentage of squares that contain differentiated cells out of the culture area.

spreadsheets (Microsoft Co., Redmond, Washington, USA). At the completion of the mapping process, computer diagrams of the distributions of the LOA grades are generated for further analyses.

Percentage area populated by adipocytes. Another variable which was analyzed is the percentage area populated by adipocytes (PAPBA). PAPBA is the percentage of squares that contain differentiated cells (i.e., with a LOA grade other than zero, at the entire culture area). The PAPBA value is calculated for each culture using the following equation [Equation (2)]:

$$\mathrm{PAPBA}[\%] = \frac{\sum_{i=1}^{4} N_i}{N} \cdot 100, \qquad (2)$$

where N_i is the number of squares with LOA grade i and N is the total number of squares.

All analyses were performed using a sample size of three different cultures. For each time point (days: 9, 12, 16, and 19 after differentiation induction), the average and standard error of the LOA and PAPBA parameters in each of the three cultures were calculated.

Micro-Scale, Monitoring Adipocyte Differentiation at the Single-Cell Level

The cultures were digitally photographed (DS-Fi1 camera; Nikon, Tokyo, Japan) using a phase-contrast microscope (Eclipse TS100; Nikon) at a microscope magnification of ×400 (FOV of

https://doi.org/10.1017/S1431927618015520

$220 \times 165\,\mu m^2$). Images were taken every 3–4 days, starting one day after the cells were seeded (days: 0, 9, 12, 16, and 19 after differentiation induction). We used triplicates of cultures ($n = 3$) and the experiment was repeated twice.

Image-Processing Algorithm and Data Analysis

A custom-made MATLAB (MathWorks, Natick, Massachusetts, USA) code was developed for extracting the LD and cell morphology data from the digital micrographs. The algorithm of this code, provided in detail in the Supplementary Appendix, is based on a previous algorithm developed by our group (Or-Tzadikario et al., 2010); however, the new algorithm provides enhanced accuracy regarding the LDs content and the ability to quantify cell shape, which is of prime importance throughout the differentiation process from fibroblasts to mature adipocytes.

The algorithm converts a microscope image (Fig. 2a) from a red-green-blue image to a grayscale image, filters for random noise, and then converts to a binary (black/white) image (based on a predetermined threshold). The outcome of these image-processing steps is that the LDs are colored white and all other components are blackened (Fig. 2b). Artifact cavities in the LDs are filled and white structures occupying <5 pixels ($0.15\,\mu m^2$) are considered to be noise, and are therefore blackened as well[1] (Fig. 2c, Or-Tzadikario et al., 2010).

In the present algorithm, an overlay of the binary image and the grayscale processed image is presented to the user (Fig. 2d). The overlay image allows for both LDs and cellular margins to be clearly visible. An individual cell can be manually selected by marking its exact margins based on the original image in grayscale [using the "roipoly" function in the Image Processing Toolbox of MATLAB (The Mathworks, Inc., 2016) for further calculations].

The user should select cells of two types: (*A*) clearly visible cells, where the boundaries of the cell are easily noticeable in the image, and (*B*) cells that are not clearly visible, where the cell boundaries are obscured. Cells of type *A* provide LD and cell morphology information. Because cells of type *B* are not clearly visible, the data extracted from these cells contribute to "lipid area per FOV" data only, and not to any other measurements. By using a customized graphical user interface in MATLAB, a user may distinguish and make a selection from these two photographed cell types.

Final outcome measures, obtained per each experimental condition and time point, were as follows:

Cell morphological parameters.

i. Cell projected area—the area contained in the marked region representing the cell, automatically calculated in pixels and converted to μm^2.
ii. Cell circularity—measure of how closely the shape of the marked region approaches that of a circle. Circularity can be valued between 0 and 1 inclusively, where 1 is the circularity value of an ideal circle [Equation (3)].

$$\text{Circularity} = \frac{4\pi A}{P^2}, \tag{3}$$

where A is the area and P is the perimeter of the cell.

[1]The 5 pixels size was determined in preliminary studies, where employing this value in the automatic image-processing code resulted in a best match to human observations (Or-Tzadikario et al., 2010).

iii. Cell eccentricity—measurement of how close the shape of the marked region approaches that of a line or a circle. Eccentricity varies between 0 and 1 inclusively, where 0 is the eccentricity value of an ideal circle shape and 1 is the eccentricity value of a line segment [Equation (4)].

$$\text{Eccentricity} = \frac{c}{a}, \tag{4}$$

where c is the distance between the foci of the ellipse and a is the major axis length.

In realistic experimental measurements, as opposed to theory, cell circularity and eccentricity are never assigned the extreme "0" or "1" values; real values may be anywhere within that range, but: $0 < \text{circularity} < 1$ and $0 < \text{eccentricity} < 1$ always applies.

LD parameters.

i. Lipid area per FOV [Equation (5)]

$$\%\text{Lipid Area Per FOV} = \frac{N_{\text{white}}}{N_{\text{total}}}, \tag{5}$$

where N_{white} is the number of white pixels only, in marked cells, and N_{total} is the total number of pixels in a FOV.

White pixels not internalized in the marked regions representing cellular margins are not considered as being LDs and, therefore, are excluded from the calculation of this variable (the white pixels represent bright areas in the image which are clearly not LDs given that they are not located within cell bodies).

ii. Mean LD radius per cell [Equation (6)]

$$R = \sqrt{\frac{S}{\pi}}, \tag{6}$$

where S is the mean LD area per cell (for calculating S, the area of all LDs is extracted, per cell, followed by calculation of mean LD area).

iii. Number of LDs per cell—the count of LDs for each clearly visible cell is performed automatically by the image-processing code.

Measurements were calculated for all clearly visible cells and time points. The mean value and standard error of each parameter were analyzed (for each time point, the number of clearly visible cells is noted in the text below).

Additionally, a "single-cell analysis" was performed in order to examine the variance (σ) of each parameter at different time points. In the single-cell analyses, the scattering of each parameter at each day has been analyzed and compared with the scattering of the same parameter across the other time points.

For cells in experimental day 0, only the fibroblastic cell morphology parameters were calculated. In days after differentiation induction, only adipocytes were analyzed. The principals and key steps of the image-processing algorithm were verified in previous published work (Or-Tzadikario et al., 2010).

https://doi.org/10.1017/S1431927618015520

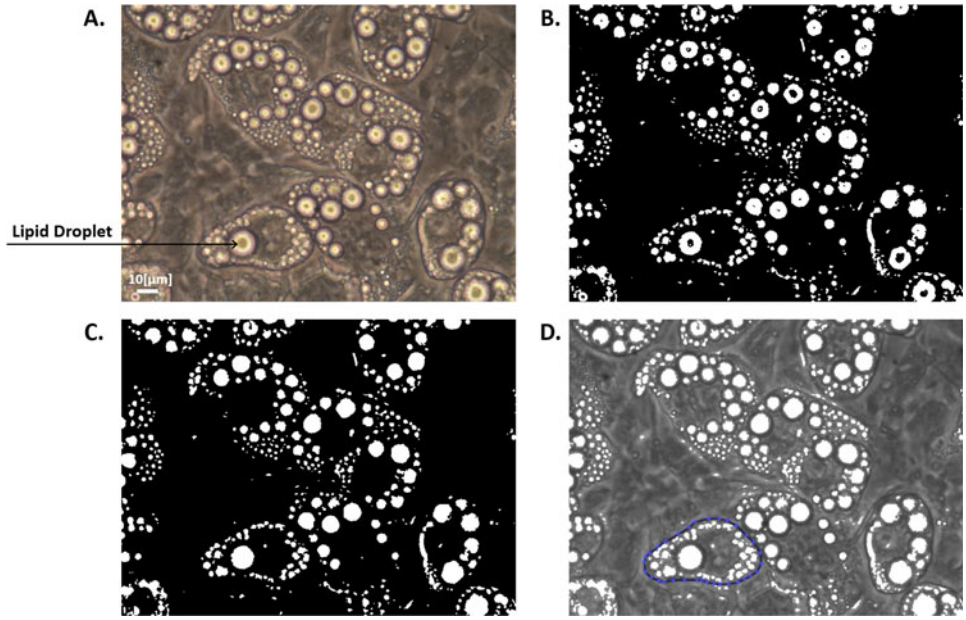

Fig. 2. Main steps in the image-processing algorithm used for monitoring adipocyte differentiation. **a**: The original image. **b**: The image is filtered for random noise and converted into a binary image. **c**: Artifact cavities in the lipid droplets are filled. **d**: Overlay of the binary image and the grayscale processed image; an individual cell is selected for further calculations.

Statistical Analysis

Statistical analysis was performed using one-way analysis of variance for the factor of time in order to identify significant changes in the values of the outcome measures, if such were detected, during the entire experimental period. A $p < 0.0001$ was considered statistically significant.

Results

Macro-Scale, Visual Differences Mapping

Mesenchymal 3T3-L1 cells were cultured and differentiated toward the adipocyte lineage. We tracked differentiation levels at different time points up to day 19 on the macro-scale using the VDM (Figs. 3a–d). The adipogenesis maps display the differentiation propagation in the culture throughout the experiment (Fig. 3a). At day 9, the differentiated adipocytes were visibly different from the fibroblastic cells based on the cell shape alteration associated with differentiation. Out of the measured area, 5% were graded "1"; as differentiation progressed, the number of squares graded "1" increased, followed by gradual increases in the "2", "3", and "4" grades since the cells continued to differentiate further as time elapsed (Fig. 3b). The analyzed LOA and PAPBA values were calculated at each time point and both increased over the experimental days, reaching 1.11 ± 0.06 and $62.65\% \pm 0.03\%$ on day 19, respectively (Figs. 3c and 3d).

Micro-Scale, Monitoring Adipocyte Differentiation at the Single Cell Level

We monitored differentiation over 19 days (Fig. 3e) and analyzed the accumulation of LDs and cell morphological changes. Before inducing differentiation (day 0, $n = 69$), the initial mean cell projected area was measured at $\sim 1{,}570\ \mu m^2$ (Fig. 3f). On day 9 ($n = 99$), when beginning of the differentiation process was observed, the cells became smaller and the mean cell projected area decreased to $\sim 380\ \mu m^2$. From that time point and onwards, the mean cell projected area increased gradually, and was measured to be $\sim 1{,}470\ \mu m^2$ by day 16 ($n = 66$) and $\sim 1{,}800\ \mu m^2$ by day 19 ($n = 99$). The single-cell analyses (Fig. 3g) clearly demonstrate that on day 9 the variance of the cell projected area parameter was the lowest ($\sigma = 244\ \mu m^2$), denoting that at the beginning of the differentiation process, the projected area of the differentiated cells was relatively uniform, and hence those cells initiated the differentiation process at the same time and were the first cells to differentiate. On the following experimental days, the variance of cell projected areas increased [e.g., day 12, $n = 71$, $\sigma = 1{,}121\ (\mu m^2)$], indicating that the projected areas of the cells in the culture was less uniform. In other words, the culture was composed of cells with small projected areas, together with cells with large projected areas, which points to variable levels of adipogenesis in the culture. It is reflected that, as the mean cell projected area initially decreased and then with LDs accumulation the mean cell projected area increased by fivefold on day 19 as compared with day 9 ($p < 0.0001$) (Figs. 3f and 3g).

As adipogenesis progressed, LDs accumulated in the cells which gradually increased. The % lipid area per FOV was <2% on day 9 and increased gradually, reaching ~18% by day 19 with a significant difference between the measured time points ($p < 0.0001$) (Fig. 3h).

The differentiation is associated with changes of cell morphology, measured by circularity and eccentricity. On day 0, where all cells are of fibroblastic shape, the mean of cell circularity value was <~0.5 (Fig. 4a), and the mean cell eccentricity value was ~0.9 (Fig. 4b), both indicating an elongated (spindle-like) cell shape. From day 9, the mean circularity value increased and stabilized at ~0.86, and the mean cell eccentricity decreased and stabilized at ~0.65. The aforementioned evolution of the circularity and eccentricity values indicate that cells were transforming from a fibroblast-like shape to a more circular shape, which are

https://doi.org/10.1017/S1431927618015520

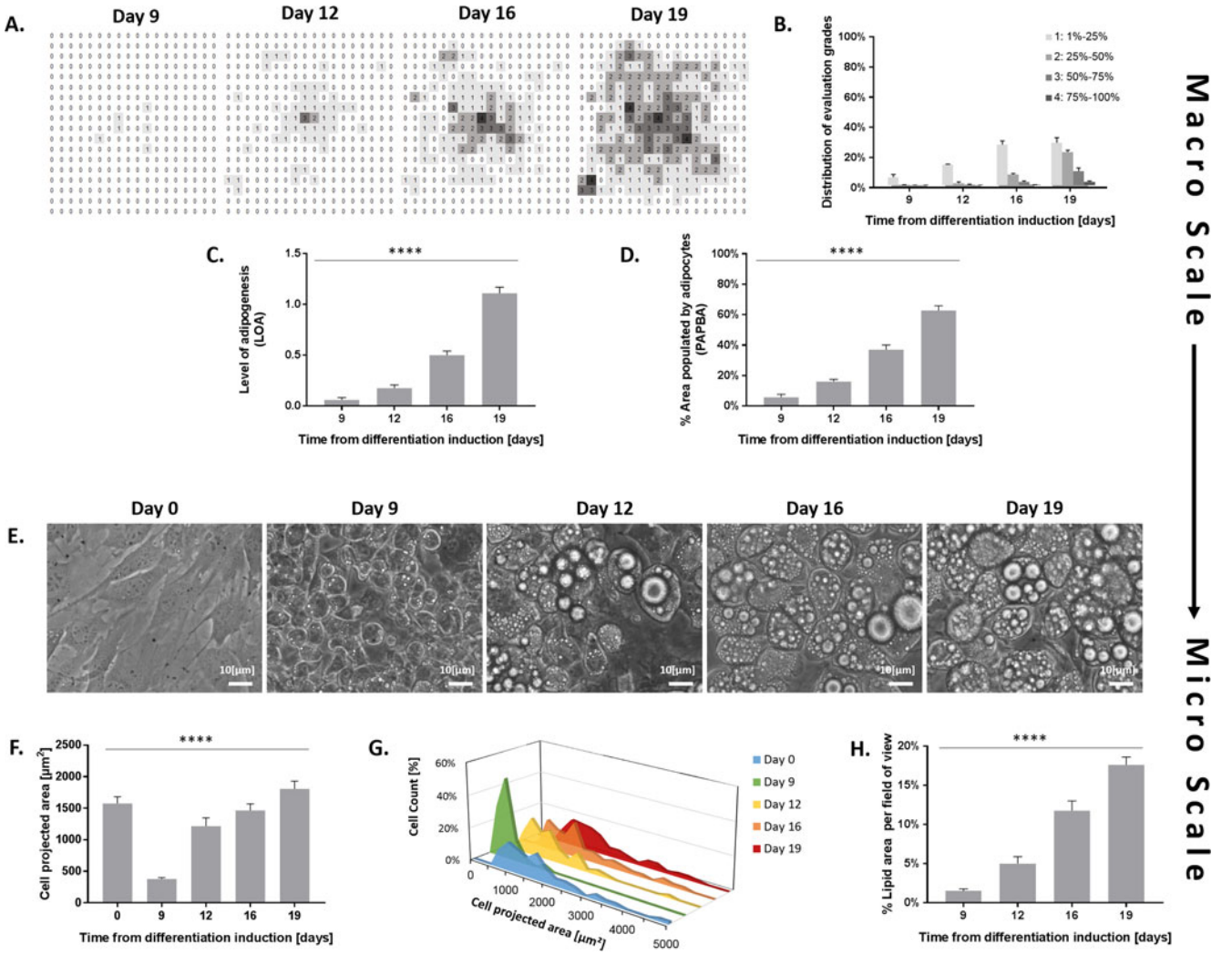

Fig. 3. Macro- to micro-scale results: (**a**) Adipogenesis maps for each time point, showing the level of adipogenesis (LOA) value in each square in the evaluation process, the maps demonstrate the progression of adipogenesis in the same culture, extracted by the visual differences mapping (VDM). **b**: Distribution of evaluation grades in the cultures, i.e. how many squares are covered by a specific evaluation value. **c**: Mean LOA value in the cultures per each time point. **d**: Mean percentage area populated by adipocytes (PAPBA) in the culture, at each specific time point. **e**: Micrographs of cell cultures seeded on glass coverslips and subjected to adipogenic differentiation at days 0, 9, 12, and 19 after differentiation induction. There are noticeable morphological changes in the cells due to the differentiation process—at the first stages of differentiation, cell projected area decrease and the cells become more circular in shape. As differentiation progresses, the cell projected area increases alongside lipid accumulation. **f**: Mean cell projected area. **g**: Distribution of the cell projected area value along the experiment. **h**: % lipid area per field of view (FOV). Error bars are the standard error, statistical significance between time points (using analysis of variance): $p < 0.0001$.

characteristic to the adipocyte lineage. Single-cell analysis of circularity and eccentricity (Figs. 4c and 4d) revealed that for the circularity value, the variance was the greatest on day 0 ($\sigma = 0.15$; dimensionless), and then gradually decreased with respect to day 0 (e.g., day 9, $\sigma = 0.13$). The variance of the eccentricity value was the lowest on day 0 ($\sigma = 0.11$), and the greatest on day 9 ($\sigma = 0.20$), and from day 9 the variance decreased (e.g., day 12, $\sigma = 0.17$). These parameters also confirm that at the onset of differentiation, the cells are rather homogenous in shape, and as differentiation progresses, additional cells differentiate; thus, the culture is less homogeneous. For both the circularity and eccentricity, there was a significant difference between days 0 and 9 ($p < 0.0001$), but the data were indistinguishable later on and the values remained relatively constant (Fig. 4).

Initial mean LD radius per cell measured on day 9 was ~1.2 μm (Fig. 5a); the value then increased gradually during the differentiation process, until reaching twofold (~2.2 μm) on day 19. The mean number of LDs measured on day 9 was 11 LDs/cell (Fig. 5b); the value then increased by fourfold on day 19 (41 LDs/cell). Single-cell analyses revealed that heterogeneity was the greatest on day 19 (Figs. 5c and 5d) for LD radius ($\sigma =$ 1.1 μm) and number of LDs ($\sigma = 27$ LDs/cell). For both values, there were statistically significant differences throughout the entire experimental period ($p < 0.0001$).

Discussion

Visual Differences Mapping

We described here the VDM, a novel method to analyze adipogenic progression in living cell cultures at the macro-scale. The adipocytes were visible in the cultures and the morphological differences in cell appearance were used to evaluate differentiation progression in the cultures. The VDM is a grid-based method,

https://doi.org/10.1017/S1431927618015520

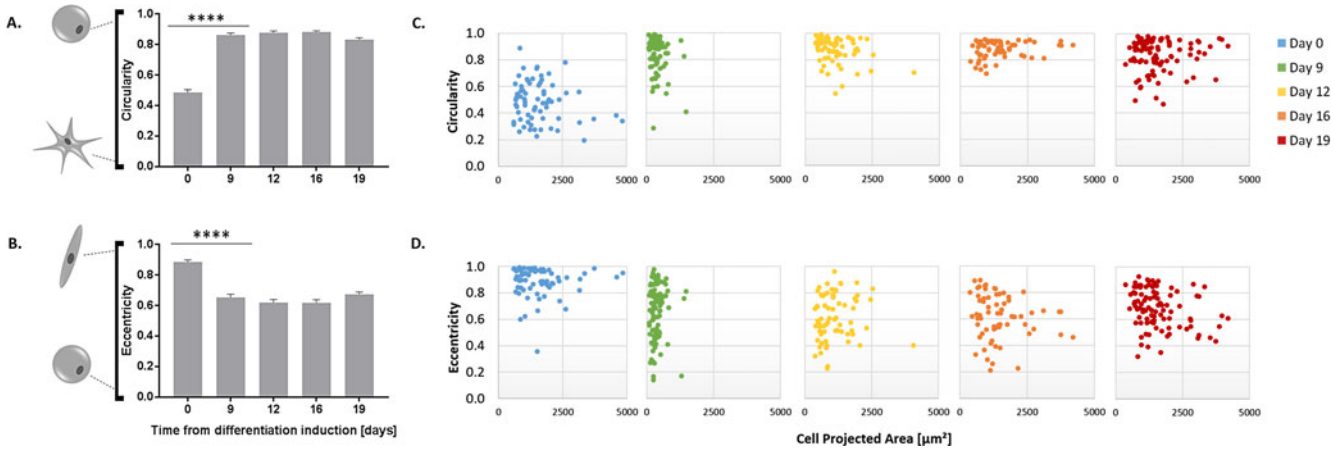

Fig. 4. Morphological parameters of the cells: (**a**) Cell circularity values. **b**: Cell eccentricity values along the time course of experiments. **c**: Single-cell analyses of circularity versus the cell projected area. **d**: Single-cell analysis of the eccentricity value versus the cell projected area. Error bars represent the standard error, statistical significance is detected between days 0 and 9 ($p < 0.0001$) using an analysis of variance; morphological data become indistinguishable post day 9.

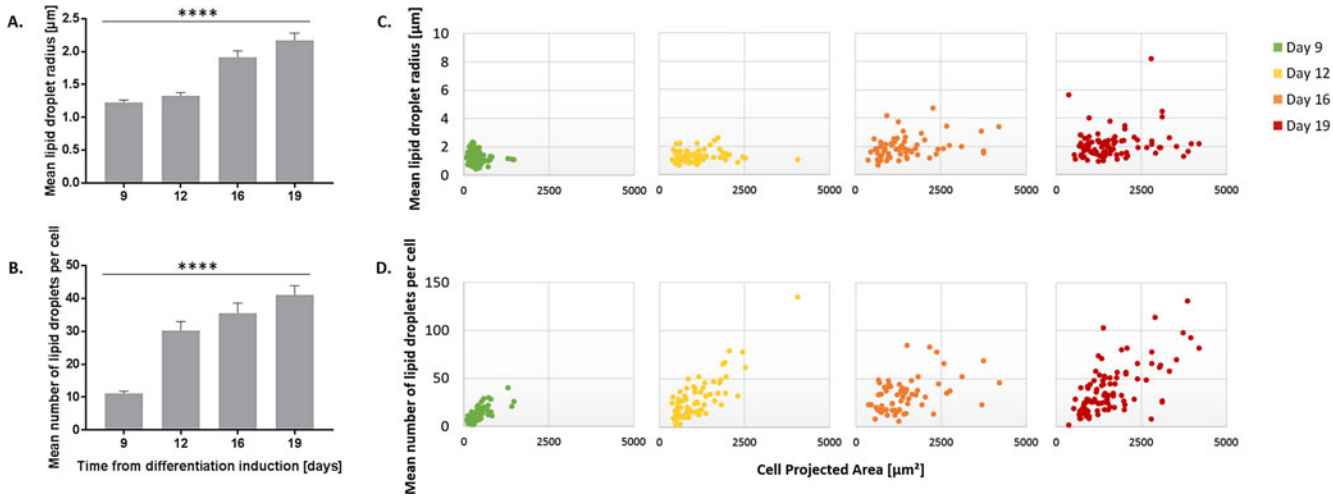

Fig. 5. Adipogenesis parameters: (**a**) Mean lipid droplet (LD) radius. **b**: Mean number of LDs per cell along the time course of experiment. **c**: Single-cell analysis of the LD radius versus the cell projected area. **d**: Single-cell analysis of the number of LDs per cell versus the cell projected area along the entire time course of experiments. Error bars represent the standard error. Statistical significance between time points is tested using an analysis of variance ($p < 0.0001$).

which is different but adopts concepts from other commonly used techniques applied in quantitative biology, e.g. a hemocytometer to determine the number of living cells in a culture (Strober, 1997) and pre-engraved gridded plates or gridded stickers (Weinmeister et al., 2008; Finlayson & Freeman, 2009; Neubrand et al., 2010; Doerner et al., 2015; Kraus et al., 2016; Macias-Romero et al., 2016; Thompson et al., 2016; Toneff et al., 2016) for locating, identifying, counting, and tracking movement of cells, cell clusters, or of other organisms. These devices are not used or provide the option to map or estimate the adipogenic propagation.

Here, we monitored the adipogenic differentiation of living cell cultures and were able to continuously quantify, for the first time in the literature, the adipogenesis of entire cultures. As expected, values of the LOA and PAPBA parameters increased during the experiment. The fundamental idea behind the VDM is that evaluation of the differentiation progression in living cultures can be measured based on morphological differences between adipocytes and fibroblasts, due to differences in their shape and LD accumulation that are observable through optical (phase-contrast) microscopy (Fig. 3). This mapping of cell differentiation states at the macro-scale facilitates continuous monitoring of the same culture at different time points and along extended periods, unlike observations performed following fixation and cell staining. Obviously, such an approach contributes substantially to the statistical power of experiments and to time/resource management. Hence, the important benefits of the VDM are its cost-effectiveness and simplicity in quantifying adipogenesis throughout the differentiation process in living cell cultures, particularly without the need for methods that compromise viability or are totally destructive.

Monitoring Adipocyte Differentiation at the Single-Cell Level

Following the macro-scale analysis of a whole culture using the VDM, we presented an enhanced image-processing algorithm, building-upon our previous work, intended for quantitative monitoring of adipocyte differentiation through measurements of LD accumulation and morphological changes at the single-cell level.

https://doi.org/10.1017/S1431927618015520

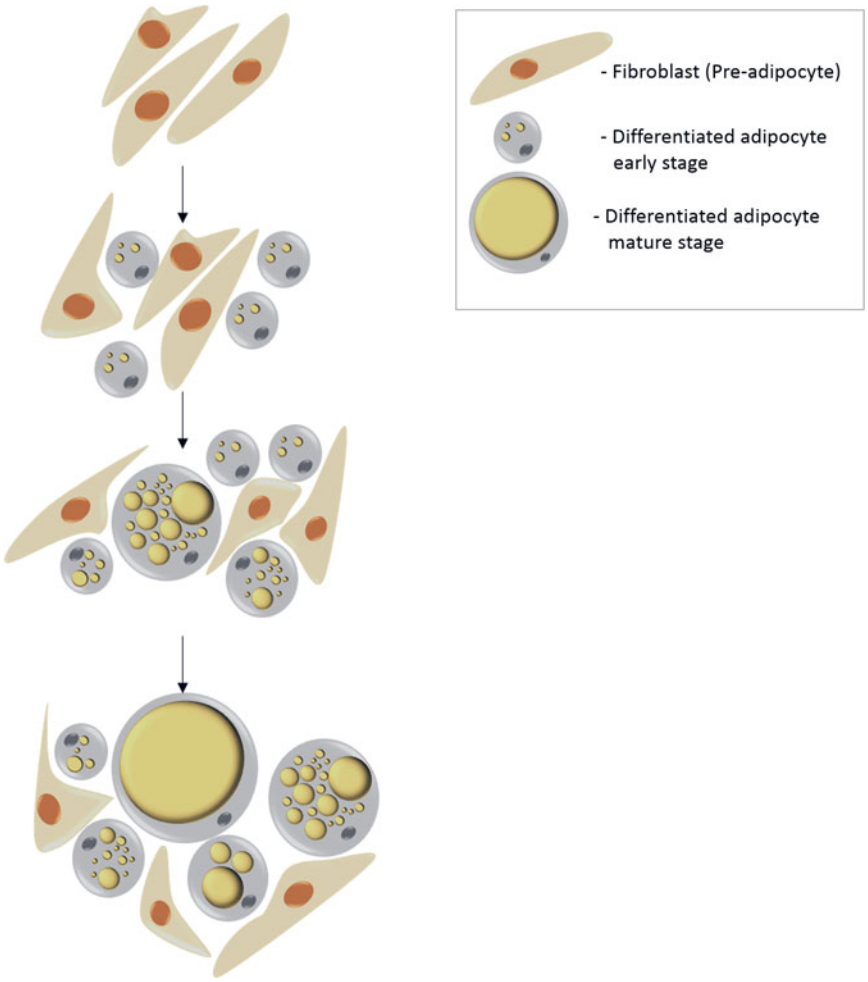

Fig. 6. Schematic illustration of differentiation in cultures exposed to adipogenic differentiation media. During the differentiation process, the cells change their shape from a spindle fibroblast-like shape to round adipocytes that acquire the spherical shape as they accumulate lipid droplets.

Other than analysis of LD accumulation which was offered by the previous algorithm (Or-Tzadikario et al., 2010), we have now added new critical features that characterize adipogenesis over time at the cell scale. The enhanced algorithm specifically facilitates analyses of intracellular parameters, such as LD size and cell morphology, which, as the present data indicate, substantially evolve as cells mature (Figs. 3–5). Hence, for the first time, the relation between LD production and cell morphological changes in individual cells can be obtained quantitatively, which adds to the innovation in this work. In addition, the parameters extracted semi-automatically from the image-processing program allow for the quantitative classification of cells, i.e. cells in primary or advanced stages of differentiation (Fig. 6), based on the single-cell analysis presented here, cell morphology and LD accumulation at different time points (Figs. 3–5).

Adipogenesis is recognized with significant morphological changes; thus, measuring such parameters of the cells is remarkably important. Cell shape changed from elongated fibroblast-like to smaller, round adipocytes with small and few LDs at the beginning of differentiation. As the experiment progressed and the LDs accumulated further, the mean cell projected area increased (Figs. 3f and 3g). The LD accumulation results presented here are in agreement with previous data published by our group (Or-Tzadikario et al., 2010; Levy et al., 2012; Shoham et al., 2012; Mor-Yossef Moldovan et al., 2018; Lustig et al., 2018*a*, 2018*b*). The lipid contents in a specific FOV increased during the differentiation process (Fig. 3h), and likewise, the mean LD radius increased (Fig. 5a). However, here we present a more precise algorithm for quantitative analysis of measurable adipogenic variables (as explained in the "Methods" section).

The results of this study demonstrate the aforementioned alterations in adipocyte morphology discussed widely in the literature, but more importantly and innovatively from a quantitative point of view, through continuous numerical evaluations of observed changes and comparisons across different time points in living cell cultures. A potential area of further study may be the use of measured morphological differences of cells cultured under various conditions or drug treatments to alter adipogenesis. The morphological parameters of adipocytes, in particular, can also provide information regarding a specific stage in the differentiation process for single cells analyzed (e.g., early or advanced differentiation, Fig. 6), as it is evident that each differentiation stage is characterized by distinct morphological properties.

Conclusions

Cell research requires the ability to distinguish between the different properties of adjacent cultured cells. In this study, we

https://doi.org/10.1017/S1431927618015520

introduced two complementary methods for continuous research of living cultures' adipogenesis. One is the VDM, at the macro-scale (of a whole culture), and the second is for micro-scale, single-cell level analyses of adipocytes, in terms of LD accumulation and morphological changes, using an image-processing algorithm. The main advantage of using these two complementary methods for the same experimental protocol is that they can be conducted in parallel, in living cultures, continuously, for extended periods of time and are not a snapshot observation. Our new approach eliminates the need for culture distortion or destruction as done by others for LD staining, gene expression detection, etc. We predict vast potential for implementation of the research approaches described here in adipose tissue-related research, such as obesity–diabetes studies, and hence we have described the experiments in great detail and included the relevant MATLAB code in the Supplementary Appendix for the research community to adopt, and perhaps develop further.

Supplementary material. The supplementary material for this article can be found at https://doi.org/10.1017/S1431927618015520

Author ORCIDs. Maayan Lustig 0000-0001-6967-0123.

Acknowledgements. We thank Ms. Y. Weinsfeld for technical assistance. This research work was supported by the Israel Science Foundation (1266/16, to DB and AG), Ministry of Science (Israel–China, 01015218 to DB and QF) and Israel–France PICS (3-12392 to AG and YP).

Author Disclosure Statement. No competing financial interests exist.

References

Ben-Or Frank M, Shoham N, Benayahu D & Gefen A (2015). Effects of accumulation of lipid droplets on load transfer between and within adipocytes. *Biomech Model Mechanobiol* **14**, 15–28. http://link.springer.com/10.1007/s10237-014-0582-8.

Choi JH, Gimble JM, Lee K, Marra KG, Rubin JP, Yoo JJ, Vunjak-Novakovic G & Kaplan DL (2010). Adipose tissue engineering for soft tissue regeneration. *Tissue Eng Part B Rev* **16**, 413–426. http://www.liebertonline.com/doi/abs/10.1089/ten.teb.2009.0544.

Choi SS, Cha BY, Lee YS, Yonezawa T, Teruya T, Nagai K & Woo JT (2009). Magnolol enhances adipocyte differentiation and glucose uptake in 3T3-L1 cells. *Life Sci* **84**, 908–914. http://dx.doi.org/10.1016/j.lfs.2009.04.001.

Deutsch MJ, Schriever SC, Roscher AA & Ensenauer R (2014). Digital image analysis approach for lipid droplet size quantitation of Oil Red O-stained cultured cells. *Anal Biochem* **445**, 87–89. http://dx.doi.org/10.1016/j.ab.2013.10.001.

Doerner JF, Delling M & Clapham DE (2015). Ion channels and calcium signaling in motile cilia. *eLife* **4**, 1–19. http://elifesciences.org/lookup/doi/10.7554/eLife.11066.

Ejaz A, Wu D, Kwan P & Meydani M (2009). Curcumin inhibits adipogenesis in 3T3-L1 adipocytes and angiogenesis and obesity in C57/BL mice. *J Nutr* **139**, 919–925. http://jn.nutrition.org/cgi/doi/10.3945/jn.108.100966.

Finlayson AE & Freeman KW (2009). A cell motility screen reveals role for MARCKS-related protein in adherens junction formation and tumorigenesis. *PLoS ONE* **4**, 1–8.

Furukawa S, Fujita T, Shumabukuro M, Iwaki M, Yamada Y, Makajima Y, Nakayama O, Makishima M, Matsuda M, Shumomura I, Shimabukuro M, Iwaki M, Yamada Y, Nakajima Y, Nakayama O, Makishima M, Matsuda M & Shimomura I (2004). Increased oxidative stress in obesity and its impact on metabolic syndrome. *J Clin Invest* **114**, 1752–1761. http://www.jci.org/articles/view/21625.

Harris LA, Skinner JR & Wolins NE (2013). Imaging of neutral lipids and neutral lipid associated proteins. In *Methods in Cell Biologyvol*, vol. **116**, Yang H and Li P (Eds.), pp. 213–226. Amsterdam, Netherlands: Elsevier.

Katzengold R, Shoham N, Benayahu D & Gefen A (2015). Simulating single cell experiments in mechanical testing of adipocytes. *Biomech Model Mechanobiol* **14**, 537–547. http://dx.doi.org/10.1007/s10237-014-0620-6.

Kraus MJ, Seifert J, Strasser EF, Gawaz M, Schäffer TE & Rheinlaender J (2016). Comparative morphology analysis of live blood platelets using scanning ion conductance and robotic dark-field microscopy. *Platelets* **27**, 541–546. http://www.tandfonline.com/doi/abs/10.3109/09537104.2016.1158400.

Levy A, Enzer S, Shoham N, Zaretsky U & Gefen A (2012). Large, but not small sustained tensile strains stimulate adipogenesis in culture. *Ann Biomed Eng* **40**, 1052–1060. http://link.springer.com/10.1007/s10439-011-0496-x.

Lin Q, Gao Z, Alarcon RM, Ye J & Yun Z (2009). A role of miR-27 in the regulation of adipogenesis. *FEBS J* **276**, 2348–2358. http://doi.wiley.com/10.1111/j.1742-4658.2009.06967.x.

Lustig M, Gefen A & Benayahu D (2018*a*). Adipogenesis and lipid production in adipocytes subjected to sustained tensile deformations and elevated glucose concentration: A living cell-scale model system of diabesity. *Biomech Model Mechanobiol* **17**, 903–913. http://link.springer.com/10.1007/s10237-017-1000-9.

Lustig M, Moldovan Mor Yossef L, Gefen A & Benayahu D (2018*b*). Adipogenesis of 3T3L1 cells subjected to tensile deformations under various glucose concentrations. In *Computer Methods in Biomechanics and Biomedical Engineering*, Gefen A and Weihs D (Eds.), pp. 171–174. Cham, Switzerland: Springer.

Macias-Romero C, Zubkovs V, Wang S & Roke S (2016). Wide-field medium-repetition-rate multiphoton microscopy reduces photodamage of living cells. *Biomed Opt Express* **7**, 1458. https://www.osapublishing.org/abstract.cfm?URI=boe-7-4-1458.

Mor-Yossef Moldovan L, Lustig M, Naftaly A, Mardamshina M, Geiger T, Gefen A & Benayahu D (2018). Cell shape alteration during adipogenesis is associated with coordinated matrix cues. *J Cell Physiol* **234**, 3850–3863. doi: 10.1002/jcp.27157.

Murphy S, Martin S & Parton RG (2010). Quantitative analysis of lipid droplet fusion: Inefficient steady state fusion but rapid stimulation by chemical fusogens. *PLoS ONE* **5**, 15030.

Neubrand VE, Thomas C, Schmidt S, Debant A & Schiavo G (2010). Kidins220/ARMS regulates Rac1-dependent neurite outgrowth by direct interaction with the RhoGEF Trio. *J Cell Sci* **123**, 2111–2123. http://jcs.biologists.org/cgi/doi/10.1242/jcs.064055.

Or-Tzadikario S, Sopher R & Gefen A (2010). Quantitative monitoring of lipid accumulation over time in cultured adipocytes as function of culture conditions: Toward controlled adipose tissue engineering. *Tissue Eng Part C Methods* **16**, 1167–1181. http://www.liebertonline.com/doi/abs/10.1089/ten.tec.2009.0755.

Patrick Jr. CW (2000). Adipose tissue engineering: The future of breast and soft tissue reconstruction following tumor resection. *Semin Surg Oncol* **19**, 302–311.

Poulos SP, Dodson MV & Hausman GJ (2010). Cell line models for differentiation: Preadipocytes and adipocytes. *Exp Biol Med* **235**, 1185–1193. http://journals.sagepub.com/doi/10.1258/ebm.2010.010063.

Qiu B & Simon MC (2016). BODIPY 493/503 staining of neutral lipid droplets for microscopy and quantification by flow cytometry. *Bio Protoc* **6**, 417–24.e5. http://www.ncbi.nlm.nih.gov/pubmed/24655651%0Ahttp://www.pubmedcentral.nih.gov/articlerender.fcgi?artid=PMC4126411%0Ahttp://www.ncbi.nlm.nih.gov/pubmed/28573161%0Ahttp://www.pubmedcentral.nih.gov/articlerender.fcgi?artid=PMC5448404.

Ramírez-Zacarías JL, Castro-Muñozledo F & Kuri-Harcuch W (1992). Quantitation of adipose conversion and triglycerides by staining intracytoplasmic lipids with oil red O. *Histochemistry* **97**, 493–497.

Ross SE (2000). Inhibition of adipogenesis by Wnt signaling. *Science* **289**, 950–953. http://www.sciencemag.org/cgi/doi/10.1126/science.289.5481.950.

Shoham N & Gefen A (2011). Stochastic modeling of adipogenesis in 3T3-L1 cultures to determine probabilities of events in the cell's life cycle. *Ann Biomed Eng* **39**, 2637–2653. http://link.springer.com/10.1007/s10439-011-0341-2.

Shoham N & Gefen A (2012*a*). Mechanotransduction in adipocytes. *J Biomech* **45**, 1–8. http://linkinghub.elsevier.com/retrieve/pii/S0021929011006622.

Shoham N & Gefen A (2012*b*). The influence of mechanical stretching on mitosis, growth, and adipose conversion in adipocyte cultures. *Biomech Model Mechanobiol* **11**, 1029–1045. http://link.springer.com/10.1007/s10237-011-0371-6.

Shoham N, Girshovitz P, Katzengold R, Shaked NT, Benayahu D & Gefen A (2014). Adipocyte stiffness increases with accumulation of lipid droplets. *Biophys J* **106**, 1421–1431. http://linkinghub.elsevier.com/retrieve/pii/S0006349514001805.

Shoham N, Gottlieb R, Sharabani-Yosef O, Zaretsky U, Benayahu D & Gefen A (2012). Static mechanical stretching accelerates lipid production in 3T3-L1 adipocytes by activating the MEK signaling pathway. *AJP: Cell Physiol* **302**, C429–C441. http://ajpcell.physiology.org/cgi/doi/10.1152/ajpcell.00167.2011.

Shoham N, Mor-Yossef Moldovan L, Benayahu D & Gefen A (2015). Multiscale modeling of tissue-engineered fat: Is there a deformation-driven positive feedback loop in adipogenesis? *Tissue Eng Part A* **21**, 1354–1363. http://www.ncbi.nlm.nih.gov/pubmed/25517541.

Steppan CM, Bailey ST, Bhat S, Brown EJ, Banerjee RR, Wright CM, Patel HR, Ahima RS & Lazar MA (2001). The hormone resistin links obesity to diabetes. *Nature* **409**, 307–312. http://www.ncbi.nlm.nih.gov/pubmed/11201732%5Cnhttp://www.nature.com/nature/journal/v409/n6818/pdf/409307a0.pdf.

Strober W (1997). Monitoring cell growth. In *Current Protocols in Immunology*, vol. **21** Appendix 3, pp. 2–3. Hoboken, NJ, USA: John Wiley & Sons, Inc. http://onlinelibrary.wiley.com/doi/10.1002/0471142735.ima03as21/full.

The Mathworks, Inc (2016) *Matlab User's Manual*. Natick, MA: The Mathworks, Inc.

Thompson GL, Roth CC, Kuipers MA, Tolstykh GP, Beier HT & Ibey BL (2016). Permeabilization of the nuclear envelope following nanosecond pulsed electric field exposure. *Biochem Biophys Res Commun* **470**, 35–40. http://dx.doi.org/10.1016/j.bbrc.2015.12.092.

Toneff MJ, Sreekumar A, Tinnirello A, Hollander P, Den, Habib S, Li S, Ellis MJ, Xin L, Mani SA & Rosen JM (2016). The Z-cad dual fluorescent sensor detects dynamic changes between the epithelial and mesenchymal cellular states. *BMC Biol* **14**, 1–16. http://dx.doi.org/10.1186/s12915-016-0269-y.

Weinmeister P, Lukowski R, Linder S, Traidl-Hoffmann C, Hengst L, Hofmann F & Feil R (2008). Cyclic guanosine monophosphate-dependent protein kinase I promotes adhesion of primary vascular smooth muscle cells. *Mol Biol Cell* **19**, 4434–4441. http://www.pubmedcentral.nih.gov/articlerender.fcgi?artid=2555919&tool=pmcentrez&rendertype=abstract.